RESEARCH BULLETIN OF THE
HIROSHIMA INSTITUTE OF TECH.
VOL. 42(2008)PP. 7-14
P A P E R

Improvement of Corrosion Fatigue Strength of WC Coated Steel by Adjusting Powder Composition and Spraying Pressure

Mitsuo KIDO* · Tarou TOKUDA* · Yoshiko SHINHARA*
Rongguang WANG* · Kozo OHOTANI** · Yuu SATAKE***

(Received Oct.1,2007)

Abstract

Two types of tungsten carbide powders, WC/Co and WC/NiCrMo, were thermally spraying coated on Mild steel by a HVOF process using two types of spray guns, models JP-5000 and DJ-2700. The spraying pressure for the JP-5000 gun was greater than the DJ-2700 gun. The corrosion fatigue behavior were investigated in 0.05kmol/m^3 of Na_2SO_4 aqueous solution for each type of coated specimen. The corrosion fatigue strength of the WC/NiCrMo specimen is higher than both the WC/Co specimens. The larger residual compressive stress was existed in the specimen prepared by the high spraying pressure than by the low spraying pressure. The corrosion resistance of the WC/NiCrMo specimens is higher than both the WC/Co specimens. The corrosion fatigue strength of the WC/NiCrMo specimen is the highest, which results from both the lower effective stress due to the larger residual compressive stress and the high corrosion resistance of the coating.

Key Words: WC thermally spraying coatings; HVOF process; spraying pressure; corrosion fatigue; residual stress; corrosion; passive film

1 Introduction

Tungsten carbides (WC) are usually used to coat steel through a high velocity oxygen-fuel flame spraying (HVOF) process to improve wear resistance (Ref 1,2). However, cracks can occur in the coating that sometimes induces delamination from the coating/substrate interface under static or cyclic tensile loads. Furthermore, aqueous solutions can penetrate to the coating/substrate interface through the defects or cracks in the coating, which induces corrosion fatigue fracture of the substrate. Until now, there have been few reports on the corrosion fatigue behavior of WC coated steel (Ref 3-5, 7). Particularly, the influence of the spraying pressure and the adjusting of the powder composition in the HVOF process has not been clearly researched.

In a previous report, the authors discussed the improvement of the corrosion fatigue strength of WC coated specimens by changing the additives in the spraying powders (Ref 3). As a result, the corrosion fatigue strength was improved by the addition of chromium in the WC/Co powder. However, the improvement effect was small and appeared only in the low stress zone. Furthermore, the spraying pressure can change the distribution of the residual compressive stress in the coated specimen (Ref 6).

In this work, two types of tungsten carbide powders were thermally spray coated on Mild steel by a HVOF process using two types of spray guns with different spraying pressures. The fatigue behavior, the corrosion behavior and the corrosion fatigue behavior were investigated and discussed.

2 Experimental Procedures

2.1 Specimens

Commercial supplied rolling steel for common structure use,

* Department of Mechanical System Engineering, Faculty of Engineering, Hiroshima Institute of Technology
** Department of Computer Science, Faculty of Applied Information Science, Hiroshima Institute of Technology
*** Graduate student, Department of Mechanical Systems Engineering, Faculty of Engineering, Hiroshima Institute of Technology

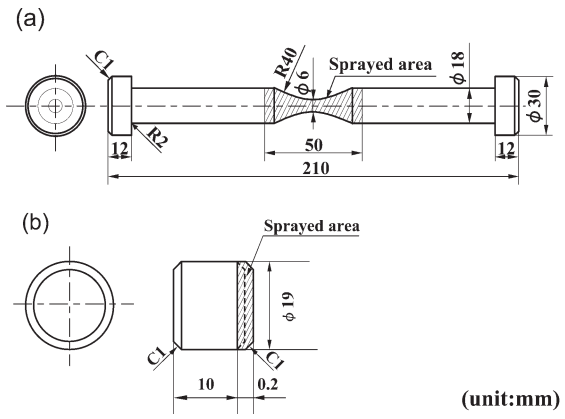

Fig.1 Shape and size of specimen (a)Fatigue test specimen, (b)Corrosion test specimen

Mild steel (Low carbon steel), was used as the substrate. The shape and size of the specimen is shown in Fig.1. The substrate was first blast processed by alumina grids and then two types of powders, WC-12mass%Co and WC-15mass%NiCrMo, were thermally spray coated by the HVOF process. The compositions of the powders are shown in Table 1. The spraying conditions are shown in Table 2. The sprayed specimens, including both the substrate and the coating, are respectively called, WC/Co-A, WC/Co-B and WC/NiCrMo-A specimens. Two spraying guns, JP-5000 and DJ-2700, were used to prepare the WC/Co-A and WC/Co-B specimens respectively, while the WC/NiCrMo-A specimen was prepared by the JP-5000 gun. The spraying pressure is greater for the JP-5000 gun than the DJ-2700 gun (Table 2) (Ref 8, 9). The thickness of each coating was about 200μm. An autograph machine (AG-250kND, Shimadzu Co., Japan) was used to obtain tensile curves at a tensile rate of 1.67x10^{-6}m/s.

Table 1 Chemical compositions of powder (mass%)

Powder	W	Ni	Mo	Cr	Fe	Co	C	O
WC/Co–A	Bal.	–	–	–	0.14	12.00	5.50	–
WC/Co–B	Bal.	–	–	–	0.09	11.90	5.33	–
WC/NiCrMo–A	Bal.	10.76	2.83	3.00	1.09	0.48	5.63	0.04

Table 2 HVOF spraying conditions

Marerial / Condition	WC/Co–A	WC/NiCrMo–A	WC/Co–B
Spray gun	JP–5000		DJ–2700
Powder size ϕ [μm]	15≦ϕ≦45		
Powder feed rate [kg/min]	0.20		0.03
Oxygen gas pressure [MPa]	1.06		1.03
Fuel gas	Kerosene		Propylene
Fuel gas pressure [MPa]	0.85		0.69
Spray distance [mm]	400		250

2.2 Fatigue Tests in Air and in Solution

In the fatigue test, a fatigue machine (SERVOPET Lab, Shimadzu Co., Japan) with a capacity of 49kN was used to produce a sinusoidally cyclic stress wave with a stress ratio of R($\sigma_{min}/\sigma_{max}$)=0 and a frequency of f=14Hz in air and in an aerated solution of 0.05kmol/m^3 Na_2SO_4 with pH=6.5. The maximum cycles were N_{max}=1.0x10^7 cycles in air and 2.0x10^7 cycles in solution. The temperature was 295±3K and the humidity was 60±10%RH during all tests. In the corrosion fatigue test, the solution was cycle flowed by a pump with a flux of 0.67mL/s and was refreshed when the specimen was changed.

2.3 Measurement of Residual Stress

The residual stress σ_R along the axis of the WC coated specimen was measured by an X-ray diffraction apparatus (M21X, Mac Science Co., Germany; XRD). The specimen was first polished with a diamond paste (mean size: 9μm) to a certain depth from the surface and then the X-ray peak of $(211)_{Fe}$ for the substrate and the peak $(102)_{WC}$ for the coating were recorded (Ref 3). Residual stress values were obtained using the parallel beam slit method, with diffraction angles determined by the half value breadth method. The stress value was calculated from the slope M of $\sin^2\psi$ curve. ψ was set for six angles at intervals of 10°(deg) between 0° and 50°. The x-ray source was Cr-Kα operated at 30kV and the anodic current was 20mA.

2.4 Measurement of Anodic Polarization and Potential Distribution

The specimens were polished by #800 emery paper and cleaned in acetone for 1.8ks before the tests. The area for the polarization was about 1x10^{2}mm^2 and the solution was aerated with 0.05kmol/m^3 of Na_2SO_4 with a pH=6.5. A potentiostat (HZ-3000, Hokuto Co., Japan) connected to a platinum plate (counter electrode) and a saturated calomel electrode (S.C.E., reference electrode) was used. The polarization test was carried out after a 0.6ks cathode reduction and 1.8ks immersion in the solution for each specimen. The current density was recorded with an increasing rate of potential of 0.83mV/s.

The potential distribution on the specimen surface in the Na_2SO_4 solution during an open circuit was measured using a scanning vibration electrode tester (SVET HV-301, Hokuto Co., Japan). The micro vibration electrode was made of Pt with a tip diameter of 20μm. The distance between the electrode and the specimen surface was set at 8μm and the scanning area was 1mm x 1mm. Before the test, a Vickers indent with cracks from the coating surface to the substrate was introduced to the

specimen as an artificial defect (Ref 10).

2.5 Surface Observation and Composition Analysis

The morphologies of the coating and the fracture of specimens after the fatigue test were observed by a scanning electron microscope (JSM-5900LV, JOEL Co., Japan; SEM). The porosity p_0 of the coating was obtained by calculating the area ratio of open pores on the observation zones of the coating.

The specimen after the SVET test was cleaned in acetone for 1.8ks and immediately analyzed by an X-ray photoelectron spectroscopy (AXIS-ULTRA, Shimadzu Co., Japan; XPS). The x-ray source in the XPS analysis was Mg-Kα. The specimen surface was sputter-etched by argon ions to get the composition change in the depth.

3 Results and Discussion

3.1 *S-N* Curves in Air

Figure 2 shows the *S-N* curves for four types of specimens in air. The stress amplitude σ_a is half the amplitude of the applied nominal stress on the cross-section of the specimen. The fatigue strength of each WC coated specimen is much smaller than the substrate. In general, the increase in the roughness of the substrate surface by the blast process for the WC coated specimens always induces a decrease in the fatigue strength. The fatigue strength of WC/Co-A specimen is a little larger than the WC/Co-B specimen. The tensile curves near the yield field of specimens are shown in Fig.3. The yield point for the WC/Co-A specimen is larger than the WC/Co-B specimen, which is a direct reason to for the higher fatigue strength for the WC/Co-A specimen than the WC/Co-B specimen. Of course, the porosity in the coating will also influence the fatigue strength. The porosity of each coating will be described in Fig. 8.

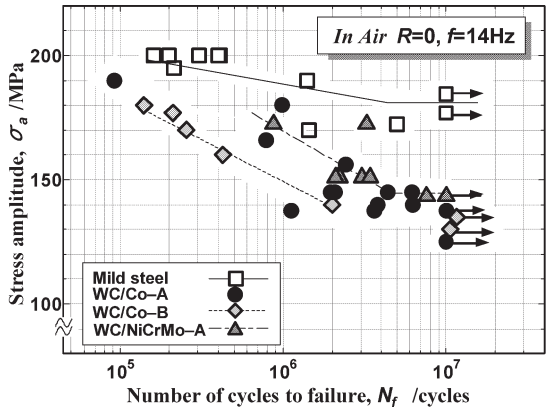

Fig.2 Relation between stress amplitude and number of cycles to failure in air.

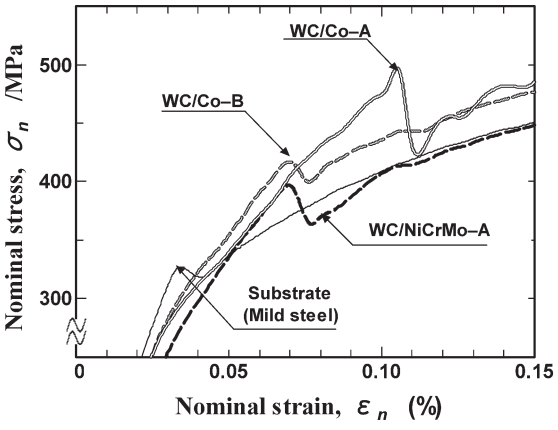

Fig.3 Relation between nominal stress and nominal strain

Figure 4 shows the distribution of residual stress σ_R along the axis of specimens from the specimen surface to the deep of the substrate. The vertical axis shows the residual stress with "+" for the compressive one and "−" for the tensile one, and the horizontal axis shows the depth from the surface to the deep of the substrate. A compressive stress is detected for each type of spraying coated specimens. The value is larger for the WC/Co-A and the WC/NiCrMo-A specimens than the WC/Co-B specimen. Especially, the larger compressive stress exists not only in the coating but also in the substrate for the WC/Co-A and the WC/NiCrMo-A specimens. The residual compressive stress in the spraying specimens will result in a decrease in the effective stress level comparing with the nominal stress (Ref 13). It will be the main reason for the increase in the yield point and the fatigue strength of the WC/Co-A specimen. The residual compressive stress was formed during the thermal spraying of the WC particles. Higher spraying pressure causes higher compressive stress in the specimen due to the collision of the

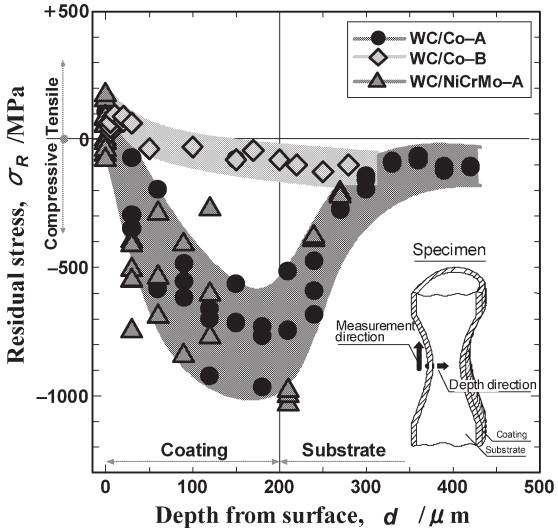

Fig.4 Distribution of residual stress in radius (depth) direction from surface

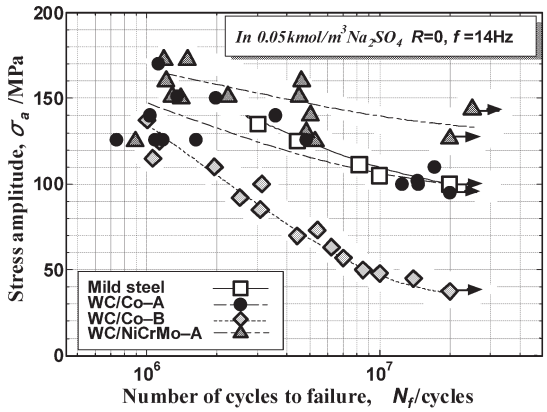

Fig.5 Relation between stress amplitude and number of cycles to failure in 0.05kmol/m³ Na_2SO_4 solution.

spraying particles to the substrate (Ref 11, 12).

3.2 *S-N* Curves in Solution

Figure 5 shows the *S-N* curves obtained in aqueous Na_2SO_4 solution. The corrosion fatigue strength of the WC/Co-B specimen is much smaller than the substrate, while the corrosion fatigue strength of WC/Co-A is almost the same as the substrate. Since the powder composition for the WC/Co-B specimen and the WC/Co-A specimen is the same, the different corrosion fatigue strength for the two specimens is clearly resulted from the difference spraying process. That is, the higher spraying pressure brings about low porosity, higher compressive stress and higher yield point for the WC/Co-A specimen, which improves the corrosion fatigue strength of the WC/Co-A specimen. According to Fig. 5, the corrosion fatigue strength of the WC/NiCrMo specimen is the largest one among specimens, and the value is much larger than the substrate. The result should be related to both the spraying pressure and the composition of the spraying powder.

Figure 6 shows micro-pits on fractured surfaces of WC coated specimens after corrosion fatigue test. Cracks are initiated from corrosion pits (Ref 14). The pits were formed by the corrosion reaction between the substrate and the solution penetrated through defects or cracks in the coating. The formation of pits is related to the corrosion resistance of the WC coated specimens including the corrosion resistance and the porosity of the coating. Figure 7 shows the polarization curves of the WC coated specimens in the Na_2SO_4 solution. The corrosion current density of each WC coated specimen is smaller than the substrate, meaning that the corrosion resistance of the WC coating is higher than the substrate. The current density of the WC/Co-A specimen is almost the same as the WC/Co-B specimen and the current density of the WC/

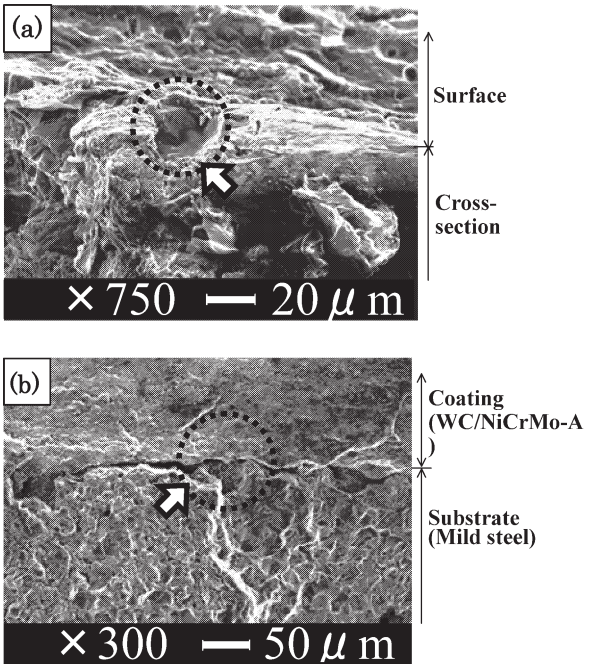

Fig.6 SEM observation of near the crack initiation point on corrosion fatigue fracture surface (Arrow indicates corrosion pits) (a)Mild steel (σ_a=115.5MPa, N_f=8.20x10⁶), (b)WC/NiCrMo-A (σ_a=126MPa, N_f=1.70x10⁷).

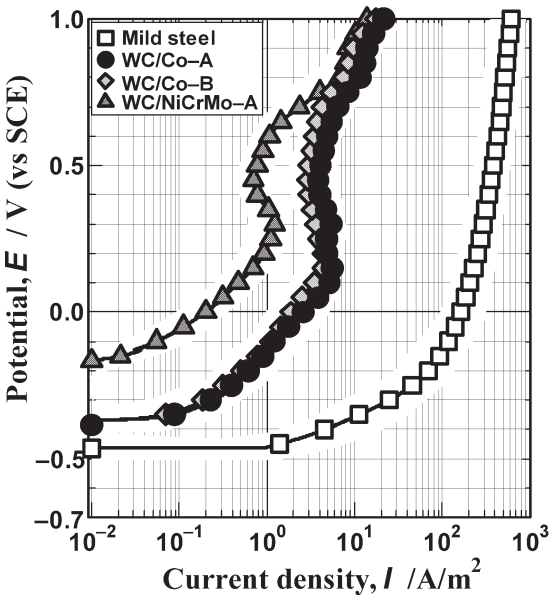

Fig.7 Polarization curve of Mild steel and WC cermet sprayed coatings in 0.05kmol/m³ Na_2SO_4 solution

NiCrMo-A specimen is much smaller than the WC/Co specimens. The highest corrosion resistance of the WC/NiCrMo-A specimen should be attributed to the formation of a compact passive film on the coating surface (Ref 15-17). On the other hand, the influence of the spraying pressure cannot be found on the corrosion resistance of the WC/Co-A and WC/Co-B specimens. In general, defects such as pores and micro-cracks exist in the coating, thus aqueous solution can penetrate to the inter-

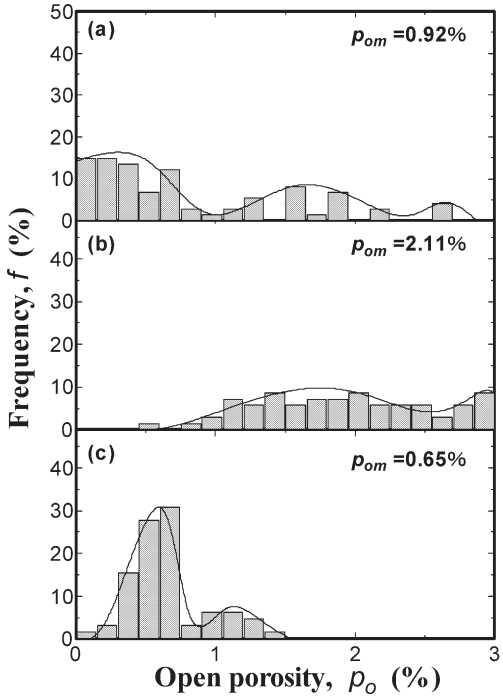

Fig.8 Open porosity of WC cermet sprayed coatings surface

face through the defects to cause pitting corrosion. Figure 8 shows the mean value of porosity (p_{0m}) of the WC coated specimens and their distribution in size (p_0). As the result, the porosity for the WC/Co-A and WC/NiCrMo-A specimens is smaller than the WC/Co-B specimen, which is attributed to the higher spraying pressure for the two specimens. Thus, the penetration of aqueous solution to the interface will become difficult for the WC/Co-A and WC/NiCrMo-A specimens than the WC/Co-B specimen. It should have influence the corrosion behavior of the WC/NiCrMo-A specimen.

Although it is believed that a compact passive film can be formed on the WC/NiCrMo-A specimen, the formation behavior of the passive film has not been clear. In order to clarify this, the potential distribution in the solution near the specimen surface at open circuit was investigated by using a scanning vibration electrode method and the result is shown in Fig.9. Before the test, a Vickers indent (P=490N, 30s) with artificial cracks from the coating surface to the interface was introduced to simulate defects in the coating. The formation of cracks by this method has been confirmed in previous papers (Ref 18). The vertical axis (Ax) shows the amplified output of the potential gradient in the solution near the specimen surface, where the plus value shows the anode area and the minus value shows the cathode area. X and Y-axis show the scanning area of 1mm x 1mm. On the WC/Co-A and the WC/Co-B specimens, anodic

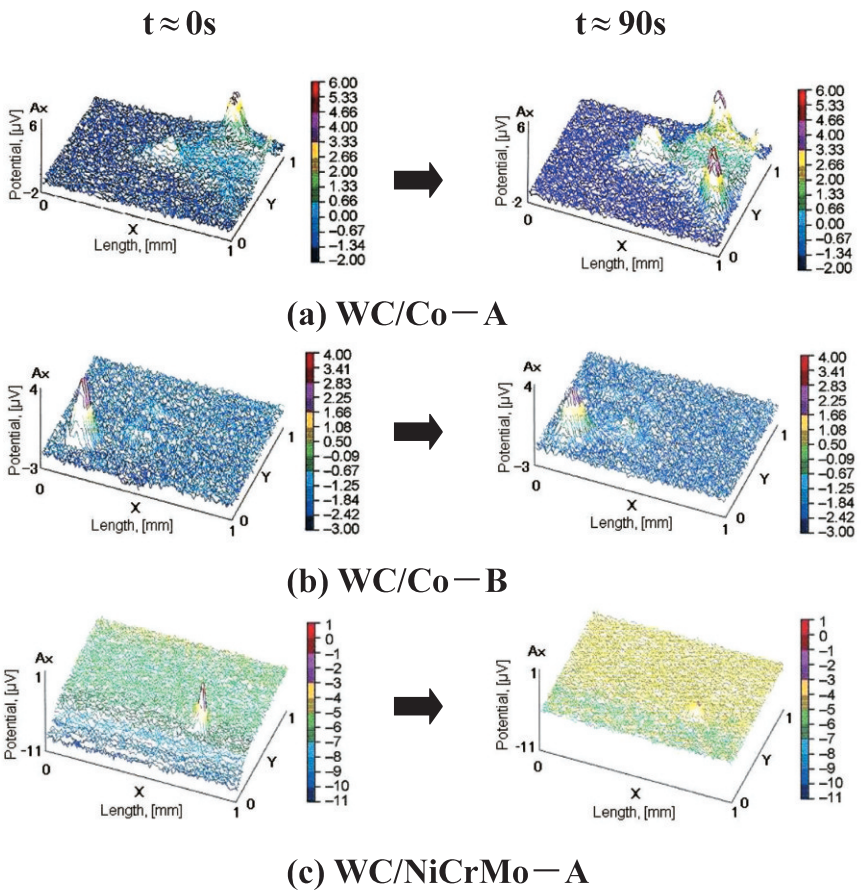

Fig.9 Corrosion potential change around the indentation of WC cermet sprayed coatings.

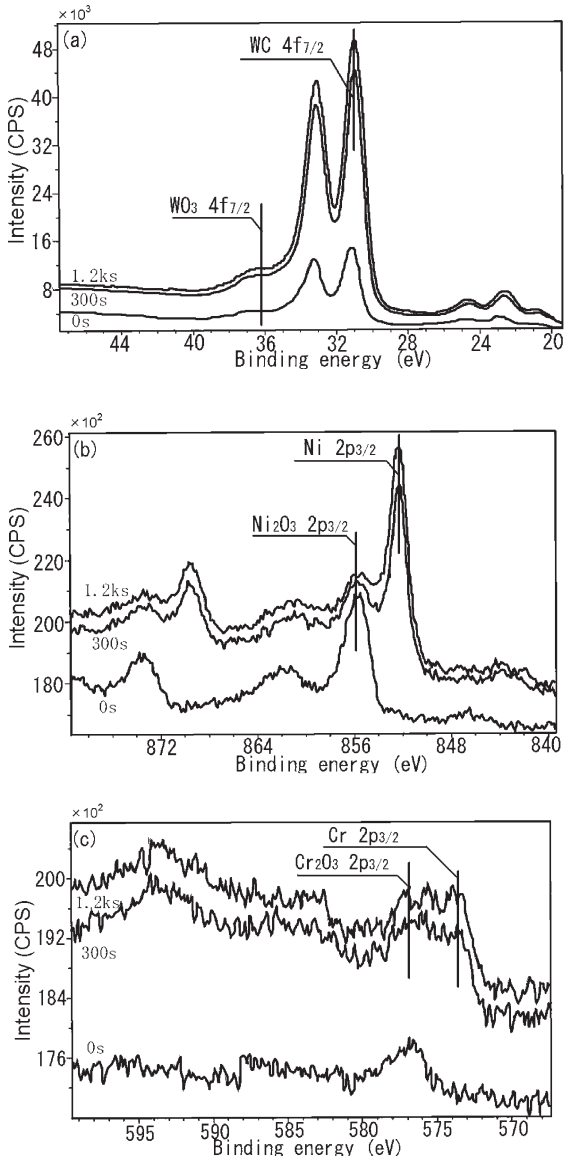

Fig.10 Spectra of Material WC/NiCrMo-A in 0.05kmol/m^3 Na_2SO_4 solution (a)W 4f spectra, (b)Ni 2p spectra, (c)Cr 2p spectra.

zones appeared near the indent after immersion (t≃0s) and the values kept stable even after t≃9ks. On the WC/NiCrMo-A specimen, the anodic zones disappeared after t≃9ks immersion, which should be attributed to the formation of passive film on the specimen surface during corrosion. The compact passive film suppresses the anodic reaction of the substrate through defects (cracks).

The composition of the passive film after the open circuit immersion test was immediately analyzed by XPS. The spectra from the WC/NiCrMo-A specimen are shown in Figure 10. The etching time of the surface by Ar^+ is indicated as $E_{t.c.t.}$ According to Fig.10 (a), W 4f peak appeared near 31.4eV and 35.5eV, corresponding to the WC and WO_3 respectively. However, the WO_3 peak is much small (Ref 18), decreases largely after Ar^+ etching, and disappeared after $E_{t.c.t}$=300s etching. Accordingly, the amount of the WO_3 in the film is small and thin. On the other hand, the Ni 2p peak appeared near 852.7eV and 855.6eV (Fig. 10(b)), corresponding to Ni^0 and $Ni(OH)_2$. After $E_{t.c.t}$=300s etching, $Ni(OH)_2$ peak largely decreased leaving only the Ni^0 peak, indicating the hydroxide of nickel is also small and thin. On the other hand, the Cr 2p peak is shown in Fig. 10(c) near 576.7eV, corresponding to Cr_2O_3. Different from that of Ni 2p and W 4f, the peak of Cr 2p almost not changed even after $E_{t.c.t}$=1.2ks etching. Furthermore, Mo 3d (Mo^0) appeared after $E_{t.c.t}$=300s etching and increased after $E_{t.c.t}$=1.2ks etching. Therefore, the passive film formed on the specimen surface should be mainly the Cr_2O_3 and Mo with a small amount of $Ni(OH)_2$. Such film plays an important role on the suppression of the corrosion of the specimen, which is related to the improvement of the corrosion fatigue strength of the WC/NiCrMo-A specimen.

3.3 Factors Related to Corrosion Fatigue Strength

As described above, the corrosion fatigue fracture is caused by both the mechanical and chemical destructions, i.e., corrosion pit forms in the substrate due to the electrochemical reaction and fatigue cracks originate from the bottom of the pit mainly due to the stress concentration (Ref 14, 19).

Comparing with the WC/Co-B specimen, the larger spraying pressure for preparing the WC/Co-A specimen and the WC/NiCrMo-A specimen brings about the larger compressive stress in the specimens and smaller porosity in the coatings. The lager compressive stress resulted in the improvement of the yield point and the fatigue strength of the specimens in air because the slip deformation of the specimens is difficult and the effective stress applied on the specimen can be decreased. The porosity also plays a role in the improvement of the yield point and the fatigue strength.

The influence of the spraying pressure for the WC/Co-A specimen and the WC/Co-B specimen did not appear in the corrosion resistance. It means that the compressive residual stress and the smaller porosity for the WC/Co-A specimen cannot largely influence the corrosion behavior of the specimen. On the other hand, the largely enhancement of corrosion resistance of the WC/NiCrMo-A specimen is attributed to both the larger compressive stress in the specimens and the formation of compact passive film with the main composition of Cr_2O_3 and Mo. The compact passive film should the mainly inhibit the penetration of solution to the coating/substrate interface and suppress the formation of the corrosion pits.

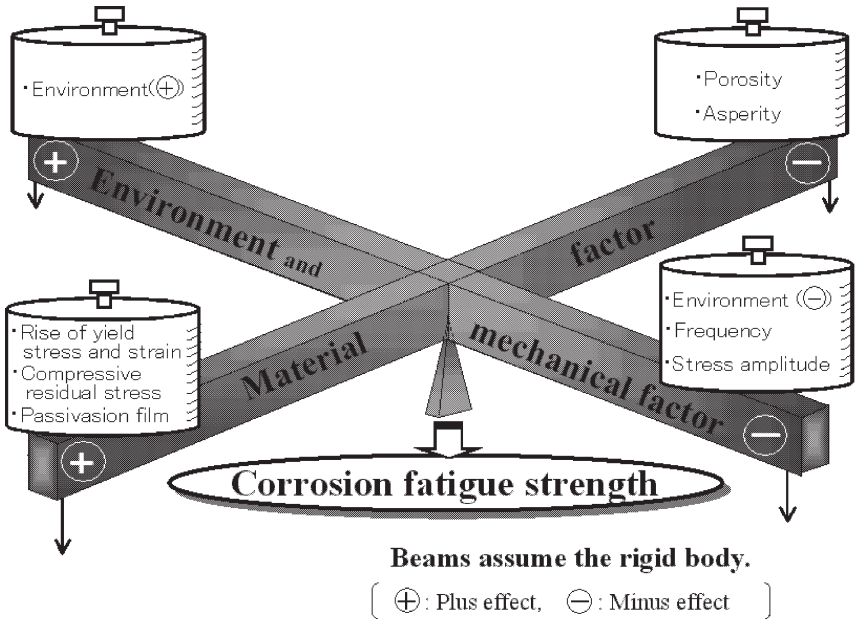

Fig.11 Various factor on corrosion fatigue strength of thermal sprayed coatings

The above factors related to the corrosion fatigue strength of specimens in this work are concluded in Fig.11. First, the compact passive film, few open pores and compressive residual stress work as the plus material factors, the asperity works as the minus environment factor (Ref 3). Next, the stress amplitude and frequency work as the minus mechanical factor, and the corrosion environment works as the minus environment factor. However, the corrosion fatigue strength is finally determined by the relative intensity of the above factors. As the experiment result, the corrosion fatigue strength of the WC/NiCrMo-A specimen is the highest one, which is attributed to the decrease of the effective stress by the large compressive stress, the formation of the compact passive film on the surface and the smaller porosity in the coating (Ref 20).

4 Conclusion

Two types of tungsten carbide powders, WC/Co and WC/NiCrMo, were thermally spraying coated on Mild steel by a HVOF process using two types of spraying guns, models JP-5000 and DJ-2700. The spraying pressure for the JP-5000 gun was greater than the DJ-2700 gun. For each type of coated specimen, the tensile curve and the fatigue behavior were first investigated in air, and then the corrosion behavior and the corrosion fatigue behavior were investigated in 0.05kmol/m^3 of Na_2SO_4 aqueous solution. The obtained conclusions are as follows.

(1) In air, both the yield stress and the fatigue strength are larger for the WC/Co-A specimen than the WC/Co-B specimen. This is attributed to the larger residual compressive stress and the smaller porosity in the specimen prepared by the higher spraying pressure (JP-5000 gun) than by the lower spraying pressure (DJ-2700 gun). The fatigue strength of the WC/NiCrMo specimen is higher than both the WC/Co specimens.

(2) The corrosion resistance of the WC/NiCrMo specimens is higher than both the WC/Co specimens. This is due to the formation of compact passive film containing Cr_2O_3 and Mo on the WC/NiCrMo specimen surface.

(3) The corrosion fatigue strength of the WC/NiCrMo specimen is the highest, which results from both the lower effective stress due to the larger residual compressive stress, and the high corrosion resistance of the coating.

Acknowledgements

Part of this work was supported by MEXT.HAITEKU, 2004～.

References

1) Y.Harada, "Thermal spraying technique and applied product of recent", Japan Inst. Metals, 1992, **31**(5), p413-421 (in Japanese).

2) K.Nakasa, M.Kato, D.Zhang and F.Egawa, "Effect of corrosive environment on the delamination strength of WC-Co coating deposited by high-velocity flame spraying", J. Soc. Mater. Sci.,Japan, 1998, **47**(2), p204-207 (in Japanese).

3) M.Kido, M.Takeda, T.Hatakenaka, K.Mukai and Y.Harada, "Corrosion fatigue fracture behavior of WC cermet sprayed mild steel", J. Soc. Mater. Sci., Japan, 2004, **53**(11),

p1228-1233 (in Japanese).

4) H.Nakahira, Y.Harada, K.Tani, R.Ebara and Y.Yamada, "Improvement of corrosion fatigue strength of high strength steel by thermal-sprayed (WC-Cr-Ni) cermet coating", J. Soc. Mater. Sci., Japan, 1994, **43**(490), p888-894 (in Japanese).

5) R.Ebara, S.Shigemura and T.Yamane, "Influence of plasma-sprayed coating on corrosion fatigue strength of 13Cr stainless steel", J. Soc. Mater. Sci., Japan, 1994, **43**(490), p881-887 (in Japanese).

6) M.Toyoda, "Thermal stresses of bonded joints of dissimilar materials and residual stress in thermal sprayed coatings", J. High Temp. Soc., 1991, **17**(11), p346-353 (in Japanese).

7) T.Hirano, R.Wang, M.Kido and Y.Harada, "Corrosion and fatigue of WC-Co sprayed materials", J. Jpn Thermal Spray. Soc The 81st discoursed collection, June 16-17, 2005(Osaka, Japan), Jpn Thermal Spray. Soc, 2005, p49-50 (in Japanese).

8) M.E.Aalamialeagha, S.J.Harris and M.Emamighomi, "Influence of the HVOF spraying process on the microstracture and corrosion behavior of Ni-20%Cr coatings", J. Mater. Sci., 2003, **38**(22), p4587-4596 (in English).

9) J. G. Legoux, B. Arsenault, L. Leblanc, V. Bouyer and C. Moreau, "Evaluation of four high velocity thermal spray guns using WC-10% Co-4% Cr cermets", J. Thermal Spray Tech., 2002, **11**(1), p86-94 (in English).

10) M.Takeda, T.Okabe, M.Kido and Y.Harada, "Corrosion behavior of WC thermal spray coatings in Na_2SO_4 solution", J. Jpn Thermal Spray. Soc., 2001, **38**(2), p58-64 (in English).

11) S.Tobe, "What has been clarified on residual stress of thermal spray coatings", J. Jpn Thermal Spray. Soc., 1998, **35**(1), p65-73 (in Japanese).

12) Y.Mima, "Doesn't fatigue strength by thermal spray technique", Zairyo-Kako, 1973, **4**, p71-75 (in Japanese).

13) M.P.Nascimento, R.C.Souza, W.L.Pigatin and H.J.C. Voorwald, "Effects of surface treatments on the fatigue strength of AISI4340 aeronautical steel", International Journal of Fatigue, 2001, **23** p607-618 (in English).

14) S.Shimohira, "Science and engineering of corrosion corrosion prevention (III)", J. Soc. Mater. Sci., Japan, 1968, **18**(184), p52-60 (in Japanese).

15) M.Moriya, K.Nakagawa and T.Morozumi, "Anodic corrosion of Hastelloy-C in sulfuric acid solution, Bulletin of the Faculty of Engineering", Hokkaido University, 1978, **86**, p57-65 (in Japanese).

16) Y.Takatani, T.Tomita, K.Tani, M.Inaba and Y.Harada, "Anodic polarization behavior of Cr carbide/Ni-Cr composite alloy", J. Soc. Mater. Sci., Japan, 1995, **44**(506), p1326-1331 (in Japanese).

17) Jiahe Ai, Jiang Xu, Fei He, Xishan Xie and Zhong Xu, "XPS study on double glow plasma corrosion-resisting surface alloying layer", Appl. Surf. Sci., 2003, **206**, p230-236 (in English).

18) M.Takeda, N.Morihiro, R.Ebara, Y.Harada and M.Kido, "Change of corrosion behavior with the immersion time on surface of WC thermal spray coating in Na_2SO_4 aqueous solusion", J. Jpn Thermal Spray. Soc., 2002, **39**(1), p7-12 (in Japanese).

19) K.Tokaji, T.Ogawa, J.U.Hwang, Y.Kobayashi and Y.Harada, "Corrosion fatigue behavior of a steel with sprayed coatings", J. Thermal Spray Tech., 1996, **5**(3), p420-427 (in English).

20) Y.Harada, M.Yoshida, S.Takeuchi and M.Kido, "Carbide cermet coating film materials and process of manufacture with corrosion resistance", Japan Patent, JP.2005-155228, 2005 (in Japanese).